

# Voltage controlled WDM devices in the visible spectrum: A SPICE simulation

M A Vieira<sup>1,3</sup>, M. Vieira<sup>1,2</sup>, A. Fantoni<sup>1</sup>, P. Louro<sup>1,2</sup>, M. Fernandes<sup>1</sup>

<sup>1</sup>Electronics Telecommunications and Computer Dept, ISEL, Lisbon, Portugal.

<sup>2</sup>CTS-UNINOVA, Lisbon, Portugal. <sup>3</sup>CML-Traffic Department, Lisbon, Portugal  
mv@isel.ipl.pt

## Abstract

A multiplexer is a device that combines two or more signals onto a single output without losing their specificity. This paper presents results on the applicability of a multilayered a-SiC:H heterostructures as an electrically programmable optical filters for WDM transmission over POF. An electrical model supported by a SPICE simulation is presented to give insight into the WDM device operation.

The WDM is a double pin a-SiC:H heterostructure which faces the modulated light incoming together from different beams, each one with a specific wavelength and transmission rate. The spectral sensitivity of the device is voltage controlled allowing the recovering of the input channels.

Results show that the output signal has a strong nonlinear dependence on the light absorption profile, i.e. on the incident light wavelength, frequency and intensity due to a self biasing of the junctions under certain unbalanced light generation of carriers. By switching between positive and negative voltages the input channels can be recovered or removed. So, this optical device allows to add and drop one or several channels (OADMS) in a WDM optical network and can be used in optical communications.

**Keywords:** Numerical and electrical simulations, optical devices, optical communication, multiplexing and demultiplexing applications, SPICE model.

## 1. Introduction

The current need for communication demands the transmission of huge amounts of information, which has become a driving force to the development of the optical communications.

Conventional optical communication systems use optical fibers for the transmission channel and light-emitting diodes (LEDs) or laser diodes for the transmitter. As optical fibers transmit infrared wavelengths with less attenuation and dispersion, the transmission uses this spectral range.

In order to increase the capacity of transmission and allow bidirectional communication over one strand fiber, wavelength-division multiplexing (WDM) is used [1]. This technique multiplexes multiple optical carrier optical signals on a single optical fiber using different wavelengths (colours) of the light source to encode different signals. A WDM system uses a multiplexer at the transmitter to join the signals together and a demultiplexer at the receiver to split them apart. The optical filtering devices have traditionally been etalons, stable solid-state single frequency Fabry-Perot

interferometers in the form of thin-coated optical filters. For optical communication in other spectral ranges, such as the visible spectrum, polymer optical fibers (POF) [2, 3] are preferred to the conventional optical fibers, as they exhibit less attenuation.

In comparison to glass fibers POF offer easy and cost-efficient processing and are more flexible for plug packing. POF can be passed with smaller radius of curvature and without any disruption because of larger diameter in comparison with glass fiber. These characteristics have opened possibilities for short distance communication systems. However, as the spectral window transmission lays within the visible spectrum the use of the WDM technique demands for adequate optical devices for the multiplexing/demultiplexing operations.

In this paper we present results on the optimization of multilayered a-SiC:H heterostructures either for wavelength-division multiplexing applications in the visible spectrum. Digital home appliance interfaces, home and car network and traffic control applications as well

as industrial applications are foreseen, due to the low cost associated to the a-SiC:H and POF technologies.

## 2. Device operation

### 2.1 Configuration

The element sensor is a glass/ITO/a-SiC:H (p-i-n)/ a-SiC:H(-p) /Si:H(-i)/SiC:H (-n)/ITO double heterostructure produced by PECVD. Deposition conditions are described elsewhere [4]. The thickness and the absorption coefficient of the front photodiode are optimized for blue collection and red transmittance, and the thickness of the back one adjusted to achieve full absorption in the greenish region and high collection in the red spectral one. As a result, both front and back diodes act as optical filters confining, respectively, the blue and the red optical carriers, while the green ones are absorbed across both [5].

In Figure 1 the device configuration is depicted. On the top of the figure it is displayed the recombination profiles (straight lines) under red ( $\lambda_R = 650$  nm) green ( $\lambda_G = 550$  nm) and blue ( $\lambda_B = 450$  nm) optical bias and different electrical bias (-6V < V < 0V). The generation profiles are also shown (symbols). We used a device simulation program ASCA-2D [6] to analyze the profiles in the investigated structure.

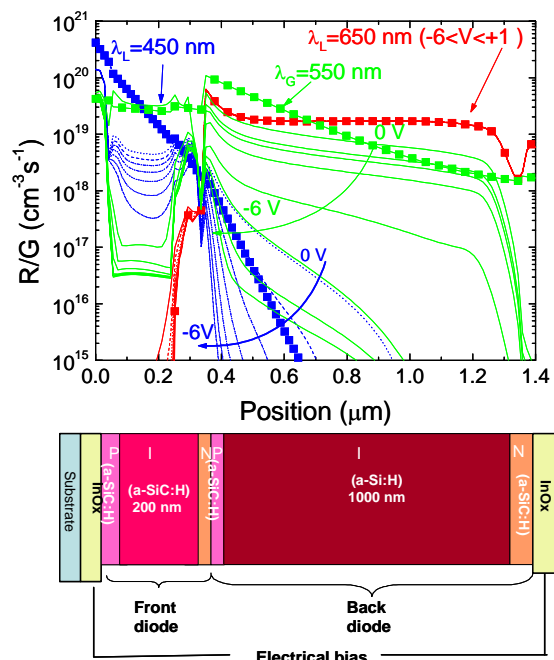


**Figure 1** a-SiC:H WDM device configuration. Recombination profiles (straight lines) under red ( $\lambda_R = 650$  nm) green ( $\lambda_G = 550$  nm) and blue ( $\lambda_B = 450$  nm) optical bias and different applied voltages (-6V < V < 0V). The generation profiles are also shown (symbols).

### 2.2 Numerical simulation

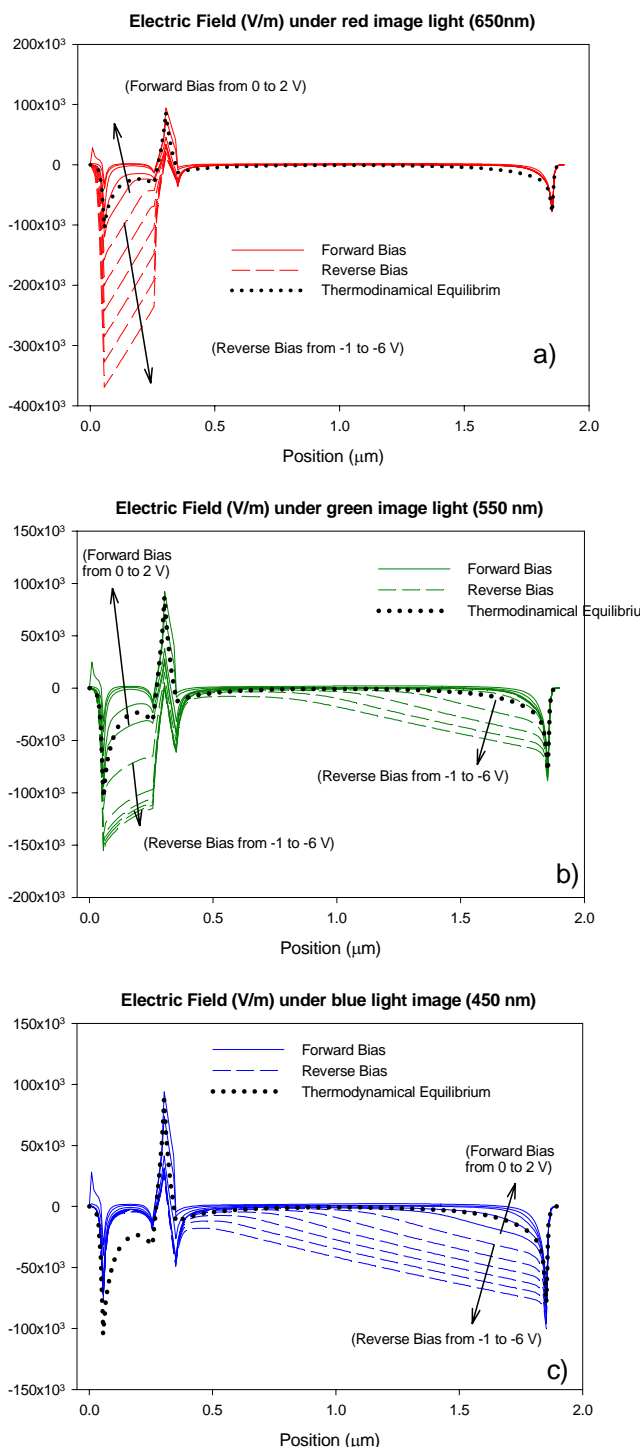


**Figure 2.** Electric field profile within the p-i-n/p-i-n tandem structure for different values of the external electrical bias and for different wavelengths of impinging light: a) 650 nm ; b) 550 nm ; c) 450 nm .

Figure 2 reports the simulated electric field profile within the p-i-n/p-i-n device for different wavelengths of the impinging light and for different values of the external electrical bias. It can be observed here the self biasing effect

under a not balanced photogeneration. When compared with the electric field profile under thermo-dynamical equilibrium conditions, the field under illumination conditions is lowered in the most absorbing cell, while the less absorbing one reacts by assuming a reverse bias configuration. Hence, opposite behaviour is observed under red and blue background light while under green light condition the redistribution of the field profile is balanced between the two sub-cells. When an external electrical bias (forward or reverse) is applied to the structure, it mainly influences the field distribution within the less photo excited sub-cell.

### 2.3 Multiplex/demultiplex device operation

Multiple monochromatic or a single polychromatic beams are directed to the device where they are absorbed, accordingly to each wavelength (Figure 1), giving rise to a time and wavelength dependent electrical field modulation across it (Figure 2) [7]. By reading out, under different applied bias, the total photocurrent generated by all the incoming optical carriers the information (wavelength, transmission rate) is multiplexed or demultiplexed and can be transmitted or recovered again.

In the multiplexing mode the device faces the modulated light incoming together from different monochromatic channels. The combined effect is converted to an electrical signal via the device.

In the demultiplexing mode a single modulated polychromatic light beam (mixture of different wavelength) each one with a different transmission rate (frequency) impinges the device and the spectral sensitivity, which is voltage controlled, allows the recognition of the different color channels.

In both modes a programmed logic circuit drive LEDs can be used to send out light into appropriated optical fibers (POF) for transmission to a destination where they can be split again using the demultiplexing mode.

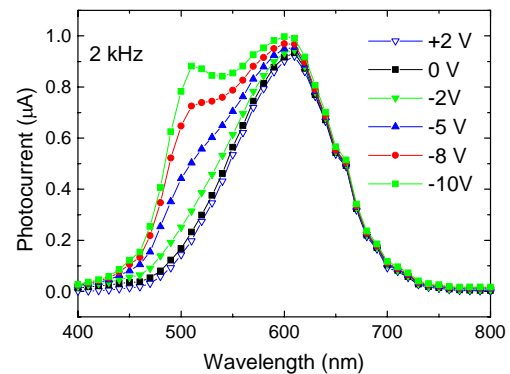
## 3. Optical characterization

### 3.1 Voltage controlled sensitivity

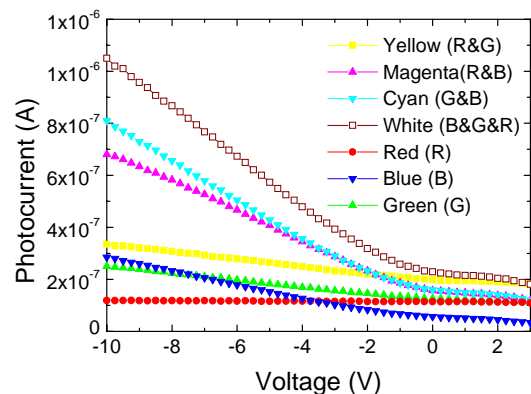
The devices were characterized at 1 kHz through spectral response (400-800nm) and photocurrent-voltage (-10V <V <+3V) measurements. In Figure 3a it is displayed the measured spectral photocurrent and in Figure 3b the *ac* current-voltage characteristics, under illumination, are shown. In this last measurement three modulated monochromatic lights: R ( $\lambda_R=650$  nm); G ( $\lambda_G=550$  nm) and B ( $\lambda_B=450$  nm),

and their polychromatic combinations; R&G (Yellow); R&B (Magenta); G&B (Cyan) and R&G&B (White) illuminated separately the device and the photocurrent was measured as a function of the applied voltage.

Results show that, as the applied voltage changes from forward to reverse the blue/green spectral collection is enlarged while the red one remains constant (Figure 3a). The photocurrent (Figure 3b) under red modulated light is independent on the applied voltage while under blue, green or combined irradiations, it increases under reverse bias.



a)



b)

**Figure 3** a) Spectral photocurrent under different applied voltages. b) *ac* IV characteristics under red (R); green (G) and blue (B), yellow(R&G); magenta (R&B); cyan (G&B) and white (R&G&B).

Results show that if the blue spectral component is present (B&R, B&G), a sharp increase with the reverse bias is observed. Under positive bias the blue signal becomes negligible and the R&B, the G&B and the R&G&B multiplexed signals overlap, respectively with the R, the G and the R&G signals. This behavior illustrates, under forward bias, the low sensitivity to the blue component of the multiplexed signal. It is interesting to notice that under reverse bias the green signal has a blue-like behavior, while under forward bias its behavior is red-like confirming the green photons absorption across both front and back diodes (Figure 1, Figure 2).

### 3.2 Linearity

In Figure 4 it is displayed the multiplexed signal obtained at reverse bias, under monochromatic light bias of different wavelengths ( $\lambda_R=650$  nm,  $\lambda_G=550$  nm,  $\lambda_B=450$  nm) and dual wavelengths combinations ( $\lambda_R=650$  nm &  $\lambda_G=550$  nm and  $\lambda_R=650$  nm &  $\lambda_B=450$  nm). The light modulation frequency of one of the light bias was chosen to be half of the other in order to ensure a synchronous relation of ON-OFF states along each cycle.

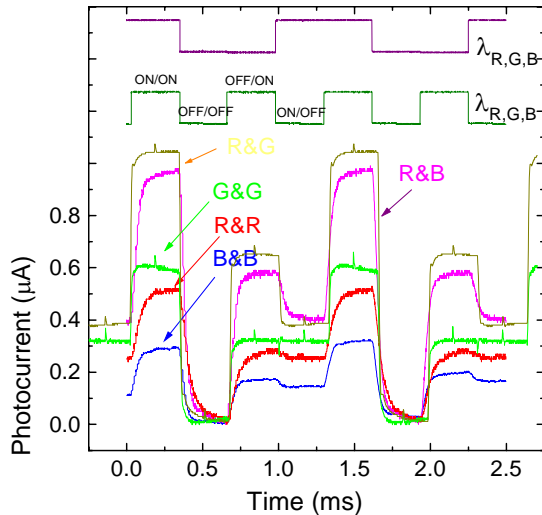


**Figure 4** Multiplexed signals at  $-5$  V and under different input light bias: R&R ( $\lambda_{R,R}=650,650$  nm); G&G ( $\lambda_{G,G}=550,550$  nm), B&B ( $\lambda_{B,B}=450,450$  nm), R&B ( $\lambda_{R,B}=650,450$  nm) and R&G ( $\lambda_{R,G}=450,550$  nm).

Under monochromatic illumination the ON-ON state corresponds to the maximum intensity of light, while the ON-OFF and OFF-ON to a lower intensity and the OFF-OFF to the dark conditions. Results suggest that for every wavelength the photocurrent signal exhibits linearity, as its magnitude is maximum in the ON-ON state, and constant in both OFF-ON and ON-OFF states (half of the observed in the ON-ON state) and minimum in the OFF-OFF state. The highest photocurrent signal under monochromatic illumination is obtained with green light ( $\lambda_G=550$  nm), followed by the red ( $\lambda_R=650$  nm) and then by the blue ( $\lambda_B=450$  nm), which is in agreement with data of Figure 3b. The multiplexed signal obtained under red and green bias ( $\lambda_R=650$  nm &  $\lambda_G=550$  nm) or red and blue bias ( $\lambda_R=650$  nm &  $\lambda_B=450$  nm) shows four different magnitude levels of photocurrent corresponding each to the conditions of states of the light bias.

### 4. Voltage sensitive wavelength division (de)multiplexing

Different wavelengths which are jointly transmitted must be separated to regain all the information. These separators are called demultiplexers.

A polychromatic time dependent wavelength combination of red, green and blue input channels with different transmission rates, were shining on the device. The transmission rate of green light component was chosen to be half of the blue and this one half of the red in order to ensure a synchronous relation of ON-OFF states along each cycle. The generated photocurrent was measured under negative and positive bias to readout the combined spectra (Figure 5).

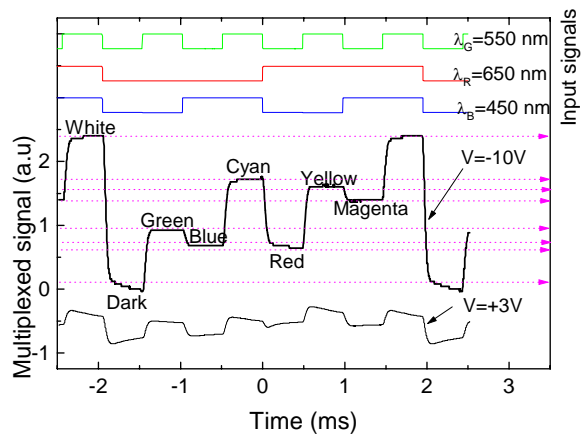


**Figure 5** Transient multiplexed signals under negative and positive bias. Polychromatic red, green and blue time dependent mixture. The digital wavelength demultiplexed signal is displayed on the top of both figures.

Results show eight distinct levels, under reverse bias. Here, the levels can be grouped into four main thresholds, ascribed respectively to the simultaneous overlap of three (R&G&B), two (R&B, R&G, B&G), one (R, G, B) and none (dark) input channels. Since under forward bias, the blue component of the multiplexed signal approaches the dark level (Figure 3) the R, the G and the R&G components are tuned. By comparing the multiplexed signals under forward and reverse bias and using a simple algorithm that takes into account the different sub-level behaviors under reverse and forward bias it is possible to split the red from the green component and to decode their RGB transmitted information. The wavelength division demultiplex signals are displayed on the top of both figures.

## 5. Electrical WDM simulation

Based on the experimental results (Figure 3, Figure 4 and Figure 5) and device configuration (Figure 1 and Figure 2) an electrical model was developed and supported by a SPICE simulation.

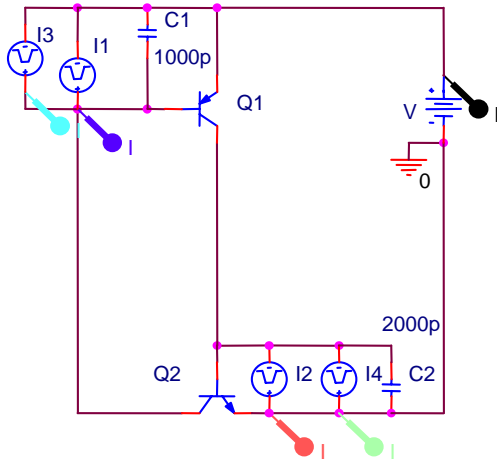


**Figure 6** Equivalent electrical circuit of the pinpin photodiode.

As displayed in Figure 7, the device is considered to be as two phototransistors connected back to back, modeling respectively the a-SiC:H p-i-n-p and a-Si:H n-p-i-n sequences. One transistor, Q1, is *npn* type and the second, Q2, *npn*. In order to simulate the n-p internal junction, the collector and base of both transistors are shared. Capacitors, C1 and C2, are used to simulate the transient capacitance due to the minority carrier trapped in both p-i-n junctions. A voltage source, V, has been applied giving rise to a current I. Two ac current sources with different frequencies, I1 and I2, are used to simulate the input blue and red channels, respectively. The green channel is simulated by two ac current sources with the same frequencies, I3 and I4, since the green light is absorbed across both front and back intrinsic layers (see Figure 1).

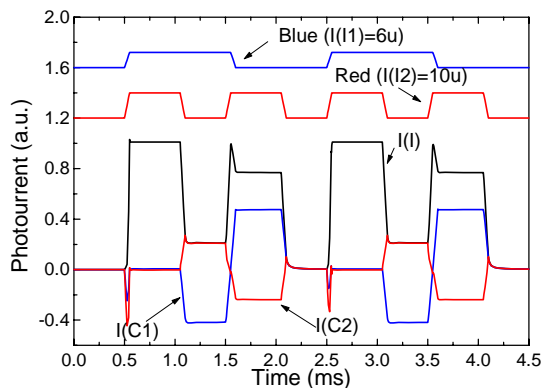


**Figure 7** Signals obtained using SPICE simulation under red (I2) and blue (I1) pulsed lights and negative applied voltages ( $V=-5V$ ).

In Figure 7 it is shown, under negative bias ( $V=-5V$ ) the input channels, I(I1), I(I2), the multiplexed signal, I(I) and the current across the capacitors, I(IC1), I(IC2).

Results show that the current, I, depends not only on the balance between both blue and red photocurrents (I1, I2) but also on the end of each half-cycle of the frequency of the modulated current. Thus, the movement of charge carriers with an increase/decrease in the irradiation, results in a charging or a displacement current similar to the current ( $i=CdV/dt$ ) that charges the capacitors. Under blue irradiation C1 charges positively and C2 negatively as a reaction to the decrease in the red irradiation. The opposite occurs under red irradiation.

In Figure 8a the simulated multiplexed signal (I(I)) due to the polychromatic mixture of three input channels, I(I1), I(I2) and (I(I3); I(I4)); is displayed under forward and reverse bias. In Figure 8b the current across C1 and C2 capacitors is shown.

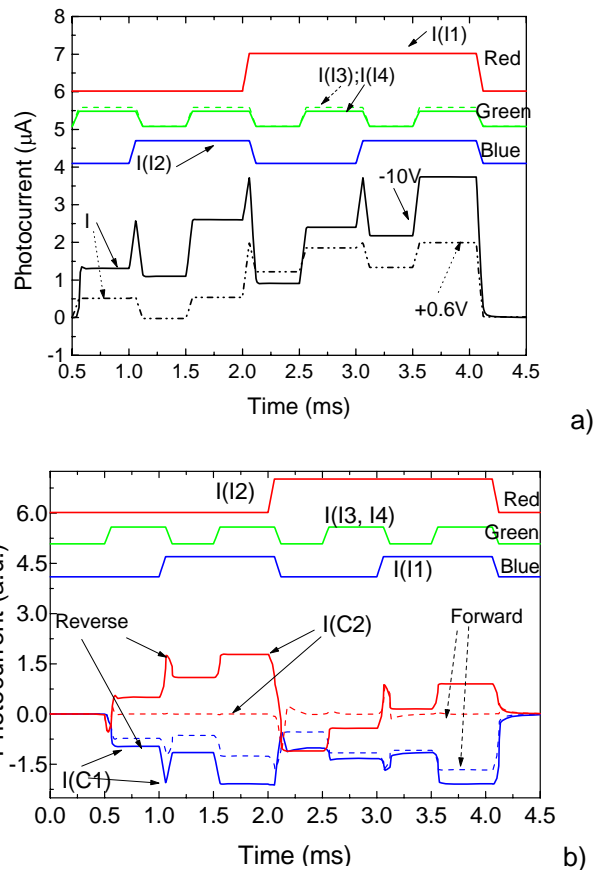


**Figure 8** a) Signals obtained using SPICE simulation under red ( $I2=20\mu A$ ), blue ( $I1=12\mu A$ ) and green ( $I3=10\mu A$ ,  $I4=8\mu A$ ) pulsed lights and different applied voltages. b) The current across the capacitors, I(IC1), I(IC2) under the same conditions.

A good agreement between experimental and simulated results is achieved (Figure 5).

As expected the external current, I, depends on the balance between blue, green and red

photocurrents (I1, (I3; I4), I2) [8] and on the end of each half-cycle of the modulated currents.

In Figure 9 it is shown the voltage drop across the base and the emitter of both Q1 and Q2 under negative and positive applied bias. If the device is biased negatively, Q1 and Q2 are in their reverse active regions. The p-n internal junction is forward-biased and the external voltage drops across both front and back reverse-biased junctions, depending on the ON-OFF state of each channel (see Figure 2). Under positive bias the internal junction is reverse-biased.

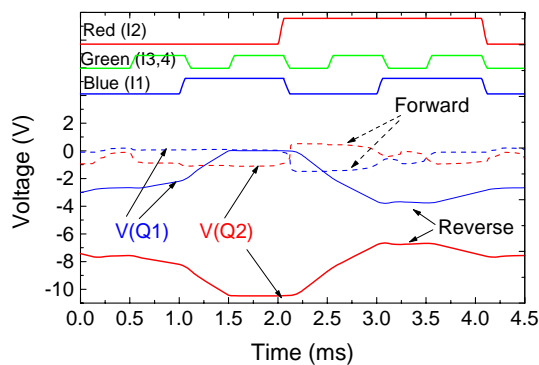


**Figure 9** a) Voltage drop ( $V_{BE}$ ) across Q1 and Q2 obtained using SPICE simulation under red ( $I_2=20\mu A$ ), blue ( $I_1=12\mu A$ ) and green ( $I_3=10\mu A$ ,  $I_4=8\mu A$ ) pulsed lights and negative and positive applied voltages.

The device acts as a charge integrator, keeping the memory of the input channels. Under reverse bias, when all the channels are simultaneously ON I1 and I3 flow across Q1 collector towards the base of Q2 and together with I2 and I4 give rise to the highest signal. When all the channels are simultaneously OFF, the current is limited by the leakage current of both active junctions (dark level). If only the blue channel is ON the carriers generated by the blue photons are injected into the base of Q1. C1 charges positively and C2 negatively as a reaction to the decrease in the red and green irradiations. The opposite occurs if only the red channel is ON. Nevertheless, if the only channel ON is the green one, both front and back contribution must be considered and the photocurrent is a balance between the blue- and the red-like contributions (Figure 1, Figure 2). If only two input channels are ON (R&B, R&G, G&B) both front and back generations are taken into account. So, once triggered (R&B&G), the device continues to conduct until the current through it drops below a certain threshold value, such as at the end of a half-cycle, keeping the information of the wavelength (R, G, B) and transmission rate (frequency) of the impinging light.

When a positive voltage is applied to turn the internal junction from ON to OFF (Figure 9), the junction capacitance across the internal n-p

junction is charged. The charging current flows through the emitter of the two transistors. The device behaves essentially as a *npn* phototransistor with the *pn*p transistor acting like a emitter-follower with a very small gain. So, under lower positive voltages, the only carriers collected come from the red and/or green channels enabling the demultiplexing of the previous multiplexed signal (Figure 5).

Comparing both the experimental and the simulated results it is observed that, under negative applied voltages, the multiplexed signal keeps the memory of the single input channels. By switching between forward and reverse bias the red, green and the blue channels were recovered.

## 6. Conclusions

Experimental and simulated results on the applicability of a multilayered double p-i-n a-SiC:H/a-Si:H heterostructures, as WDM devices in the visible spectrum, were presented.

Three modulated input channels were transmitted together, each one located at different wavelength and frequencies. The combined optical signal was analyzed by reading out the photocurrent generated across the device.

Results show that by switching between positive and negative voltages the input channels can be recovered or removed. So, this optical device allows to add and drop one or several channels in a WDM optical network (OADMS) and can be used in optical communications.

A physical model supported by an electrical and a numerical simulation gives insight into the device operation.

## References

- [1] Michael Bas, Fiber Optics Handbook, Fiber, Devices and Systems for Optical Communication, Chap, 13, Mc Graw-Hill, Inc. 2002.
- [2] Mark G. Kuzyk, Polimer Fiber Optics, Materials Physics and Applications, Taylor and Francis Group, LLC; 2007.
- [3] O. Ziemann, J. Krauser, P.E. Zamzow, W. Daum, POF Handbook, Optical Short Range Transmission Systems, Springer, 2<sup>nd</sup> Ed., 2008.
- [4] M. Vieira, A. Fantoni, M. Fernandes, P. Louro, G. Lavareda and C.N. Carvalho, Thin Solid Films, 515, Issue 19, 2007, 7566-7570.
- [5] P. Louro, M. Vieira, Yu. Vygranenko, A. Fantoni, M. Fernandes, G. Lavareda, N. Carvalho Mat. Res. Soc. Symp. Proc., 989 (2007) A12.04.
- [6] A. Fantoni, M. Vieira, R. Martins, Mathematics and Computers in Simulation, Vol. 49. (1999) 381-401.
- [7] M. Vieira, M. Fernandes, J. Martins, P. Louro, R. Schwarz, and M. Schubert, IEEE Sensor Journal, 1, 2001, 158-167.
- [8] Edward S. Yang, "Microelectronic devices", Cap. 5, Department of Electrical Engineering, Colombia University, Mc Graw-Hill, Inc. 1988.